Laminin and hyaluronan supplementation of collagen hydrogels enhances endothelial function and tight junction expression on three-dimensional cylindrical microvessel-on-a-chip

Daniel Alcaide, Baptiste Alric, Jean Cacheux, Shizuka Nakano, Kotaro Doi, Marie Shinohara, Makoto Kondo, Aurelien Bancaud, Yukiko Matsunaga

Biochemical and Biophysical Research Communications 724 (2024) 150234

Contents lists available at ScienceDirect

Biochemical and Biophysical Research Communications

journal homepage: www.elsevier.com/locate/ybbrc

Laminin and hyaluronan supplementation of collagen hydrogels enhances endothelial function and tight junction expression on three-dimensional cylindrical microvessel-on-a-chip

Daniel Alcaide [a,b,c], Baptiste Alric [a,c], Jean Cacheux [a,c,d], Shizuka Nakano [a,b], Kotaro Doi [a], Marie Shinohara [a,b], Makoto Kondo [a], Aurelien Bancaud [a,c,e,**], Yukiko T. Matsunaga [a,b,c,*]

[a] Institute of Industrial Science, The University of Tokyo, 4-6-1 Komaba, Meguro-ku, Tokyo, 153-8505, Japan
[b] Department of Bioengineering, School of Engineering, The University of Tokyo, 4-6-1 Komaba, Meguro-ku, Tokyo, 153-8505, Japan
[c] LIMMS, CNRS-IIS UMI 2820, The University of Tokyo, Tokyo, 153-8505, Japan
[d] Centre de Recherches en Cancérologie de Toulouse, Inserm, CNRS, Université Paul Sabatier, Université de Toulouse, 31037, Toulouse, France
[e] LAAS-CNRS, CNRS UPR8001, 7 Avenue du Colonel Roche, 31400, Toulouse, France

ARTICLE INFO

Keywords:
Vasculature-on-a-chip
Microvessel
Endothelial cells
Hydrogel
Collagen
Laminin
Hyaluronan
Tight junction

ABSTRACT

Vasculature-on-chip (VoC) models have become a prominent tool in the study of microvasculature functions because of their cost-effective and ethical production process. These models typically use a hydrogel in which the three-dimensional (3D) microvascular structure is embedded. Thus, VoCs are directly impacted by the physical and chemical cues of the supporting hydrogel. Endothelial cell (EC) response in VoCs is critical, especially in organ-specific vasculature models, in which ECs exhibit specific traits and behaviors that vary between organs. Many studies customize the stimuli ECs perceive in different ways; however, customizing the hydrogel composition accordingly to the target organ's extracellular matrix (ECM), which we believe has great potential, has been rarely investigated. We explored this approach to organ-specific VoCs by fabricating microvessels (MVs) with either human umbilical vein ECs or human brain microvascular ECs in a 3D cylindrical VoC using a collagen hydrogel alone or one supplemented with laminin and hyaluronan, components found in the brain ECM. We characterized the physical properties of these hydrogels and analyzed the barrier properties of the MVs. Barrier function and tight junction (ZO-1) expression improved with the addition of laminin and hyaluronan in the composite hydrogel.

1. Introduction

Vasculatures are semipermeable barriers that regulate blood–tissue exchanges [1]. Considering their critical role in drug targeting, the functions of vasculatures have received significant attention in fields such as pharmacology [2]. Because of their cost-effectiveness and ethical value in reducing the use of animal models in research, organ-on-chip technologies based on vasculature-on-chip (VoC) models have been increasingly used in preclinical testing [3]. VoCs have been fabricated using different technologies, with the most complex models assembled in a three-dimensional (3D) geometrical configuration using a biocompatible soft material. Hydrogels are physiologically similar, with collagen gels having proven their relevance in reconstituting cohesive layers of endothelial cells (ECs) [4]. To mimic more complex physiological conditions, some studies have supplemented the composition of collagen gels with materials such as fibrin or Matrigel [5,6]. However, even with supplementation, accurate replication of the intricate organ-specific extracellular matrices (ECMs) *in vitro* has not been developed. This uncertainty is further increased by the lack of evidence demonstrating whether the organ-specific characteristics of endothelial tissues arise solely from the specialization of ECs or in conjunction with biochemical and biophysical cues present in the tissue microenvironment [5].

The mechanical stimuli that ECs receive in a 3D VoC can be

Abbreviations: VoC, Vasculature-on-Chip; P_D, diffusive permeability.

* Corresponding author. IInstitute of Industrial Science, The University of Tokyo, 4-6-1 Komaba, Meguro-ku, Tokyo 153-8505, Japan.
** Corresponding author. CNRS, LAAS, 7 Avenue du Colonel Roche, 31400, Toulouse, France.
E-mail addresses: abancaud@laas.fr (A. Bancaud), mat@iis.u-tokyo.ac.jp (Y.T. Matsunaga).

https://doi.org/10.1016/j.bbrc.2024.150234
Received 22 May 2024; Received in revised form 30 May 2024; Accepted 5 June 2024
Available online 6 June 2024

modulated by manipulating the physical properties of the hydrogel [7], as well as by inducing shear stress on the ECs through the application of pressure or flow inside the vasculature [8]. The chemistry of the 3D VoC microenvironment can also be adjusted by introducing specific soluble factors into the culture medium or by coculturing ECs with other organ-specific cells [9]. Organ-specific vasculature response is best illustrated in the central nervous system with the blood–brain barrier (BBB), which is maintained by tight junctions in between ECs [10] with high size-selectivity for molecular transport. The ECM composition of brain tissue may contribute to this specific response because of its unique components, such as hyaluronan, proteoglycans, laminin and fibronectin [11]. However, very few studies have attempted to mimic cerebral blood vessels using composite materials based on type I collagen gel and other brain ECM proteins [12]. Therefore, we addressed the question of how the composition of the supporting hydrogel of a VoC influences its barrier function by recreating *in vitro* 3D cylindrical microvessels (MVs).

Here, we used collagen type I gel, hereafter referred to as "Collagen I″, and mixture of collagen I/III, laminin 111, and hyaluronan, hereafter referred to as "MatriMix". We compared their structural and physical properties and seeded two types of human ECs: namely human umbilical vein ECs (HUVECs) and human brain microvascular ECs (HBMVECs) to fabricate MVs. Finally, we assessed barrier function assay of each MV and investigated the expression of EC–EC adherent junctions and tight junctions.

2. Materials and methods

2.1. Cells

HUVECs (Lonza, Basel, Switzerland) were maintained with EGM-2 EC culture medium (Lonza). The culture medium was changed every other day, and the HUVEC culture was kept until passage number 7. HBMVECs (iXCells, San Diego, USA) were thawed and cultured in EC basal medium (iXCells). The subculture was kept until passage number 5.

2.2. MV chip preparation

We use single MV polydimethylsiloxane (PDMS) microfluidic chips and followed a surface treatment method proposed previously [13,14]. Hydrogels were prepared after the treatment of chips and needles. Collagen I hydrogel was fabricated using a mix of Cellmatrix® Type I-A 3 mg/mL collagen solution (Nitta, Osaka, Japan) with Hank's buffer and collagen buffer and phosphate-buffered saline (PBS) at a 6.7:1:1:1.3 vol ratio. MatriMix® (Nippi, Tokyo, Japan) hydrogel was fabricated by mixing the three components (hyaluronan/laminin 111 solution, $NaHCO_3$ buffer, and Collagen I/III solution) provided by the manufacturer at a 5.4:0.6:4 vol ratio. The final collagen concentration was 2 mg/mL for both hydrogels, with MatriMix containing laminin and hyaluronan at concentrations of 5 μg/mL and 0.2 mg/mL, respectively. The mixture was then added to the MV chip (10 μL in each reservoir of the chip and 30 μL in the central cavity), followed by a rapid insertion of acupuncture needle. Chips were kept in the incubator for 10 or 30 min to allow for gelation, and then the needle was removed to form the acellular channel.

2.3. MV fabrication

HUVECs and HBMVECs were seeded into the acellular hydrogel channel from both inlets at 50,000 cells each and allowed to attach to the hydrogel scaffold at 37 °C for 10 min [14]. Warm EC-specific medium was added, and MV were cultured at 37 °C until use on the third day of culture.

2.4. Characterization of hydrogel properties

To characterize the elastic modulus and permeability of hydrogels, we employed the method previously developed in Ref. [15], in which the pressure evolution on top of the hydrogel was registered upon application of a constant pressure in the range of 200–1000 Pa in the acellular hydrogel channel. Pressure kinetic changes were then analyzed with the analytical poroelastic model of ref. [15] to infer the elastic modulus and permeability.

2.5. Scanning electron microscopy (SEM)

Collagen I and MatriMix were prepared as disks with a diameter of 5 mm and a thickness of 3 mm using silicone molds. All samples were fixed with 2.5 % glutaraldehyde for 2 h at room temperature and then dehydrated by exposure to a graded ethanol series (057–00456; FujiFilm Wako; 50 %, 70 %, 80 %, 90 %, and 100 % for 30 min each). After the replacement of 100 % ethanol overnight with gentle shaking, the samples were exposed to a graded series of ethanol–*t*-butanol (ethanol/*t*-butanol: 75 %/25 %, 50 %/50 %, and 25 %/75 % for 30 min each). After the replacement of 100 % *t*-butanol twice for 30 min, the samples were freeze-dried overnight and coated with osmium. Observation was performed with a field emission scanning electron microscope (FE-SEM, JSM-7500F, JEOL, Tokyo, Japan) at 3 kV accelerating voltage.

2.6. Microscopies

Phase contrast multi-tile panoramic images of each MV were taken with an AXIO observer Z1 microscope (Carl Zeiss, Oberkochen, Germany) focusing on the equatorial plane of the MVs at 20 × . Diffusion assay time lapses and immunostaining images were taken using a confocal laser scanning microscope (CLSM; LSM 700, Carl Zeiss) using the 10 × or 20 × objective lens.

2.7. Diffusion assay

The diffusive permeability (P_D) across the MV barrier was evaluated through the simultaneous injection of two fluorescent probes of different molecular weights, fluorescein isothiocyanate (FITC)-conjugated 4 kDa average dextran (Sigma-Aldrich, Missouri, USA) and rhodamine-conjugated 70 kDa average dextran (Sigma-Aldrich), both at 10 mg/mL in 1 % PBS and mixed thoroughly, in the VoC lumen. The assay was performed using the same device and protocol described previously [14,16]. The acquisition of diffusion timelapses was performed in the span of 4 min with images captured every 3.87 s, for a total of 50 images at 10 × or 20 × magnification. The P_D calculations were obtained by analyzing the time-lapse images using ImageJ software (Maryland, USA), following the model established in our previous study [14,17].

2.8. Immunocytochemistry

MVs fixed with 4 % paraformaldehyde were then permeabilized with 1 % Triton X-100. Blocking was performed overnight at 4 °C with 1 mL of 1 % BSA. MVs were treated with primary antibodies of VE-cadherin (rabbit 2500, Cell Signaling, Boston, MA, USA) or ZO-1 (rabbit 40–2200, Thermo Fischer Scientific, Waltham, MA, USA) in 1 % BSA (1:200) overnight at 4 °C and rinsed with PBS thoroughly after. Alexa Fluor 555-conjugated goat anti-rabbit IgG secondary antibody (A-21428; Thermo Fisher Scientific) (1:1000) and Hoechst 33342 (1:1500) in 1 % BSA were added to the MVs and kept at 4 °C overnight.

2.9. Statistical analysis

Numerical values were expressed as the mean ± standard error of the mean. Statistical differences between conditions were evaluated using Student's *t*-test, with p values indicated either in the graphs or legends

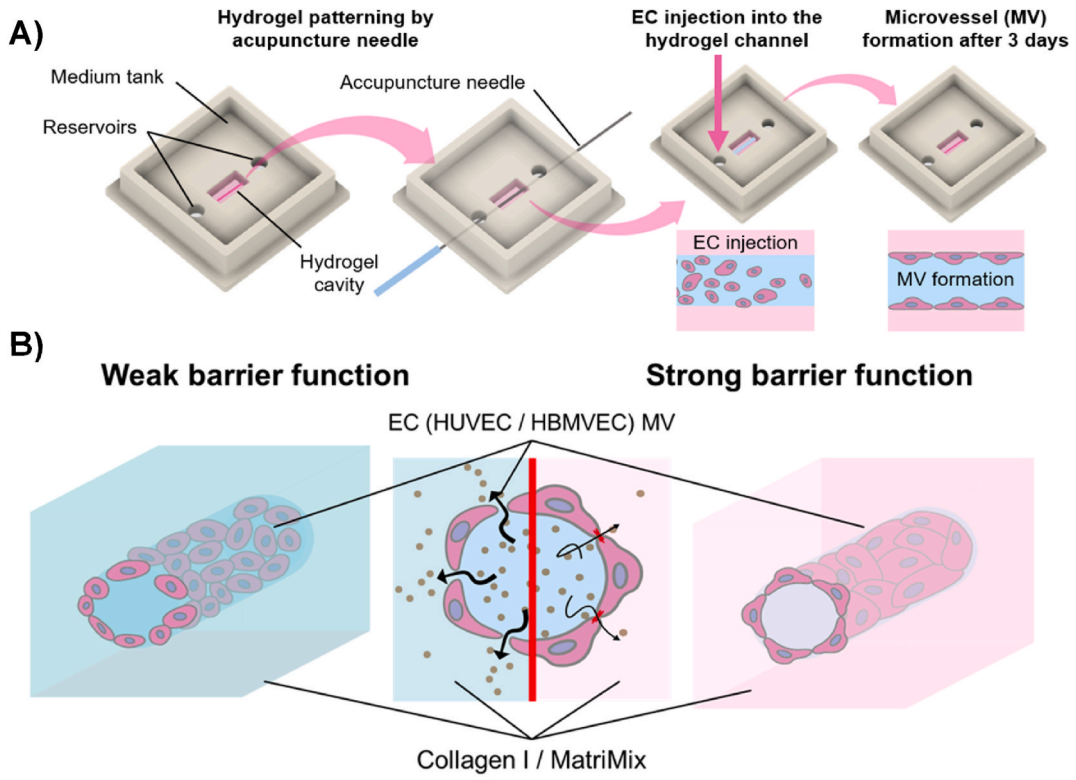

Fig. 1. Concept of this study A) Steps of MV fabrication. ECs were seeded in the hydrogel channel and cultured for 3 days for MV maturation. **B)** Barrier function assay. The responses of HUVECs and HBMVECs in two hydrogels of different compositions (Collagen I and MatriMix) were evaluated.

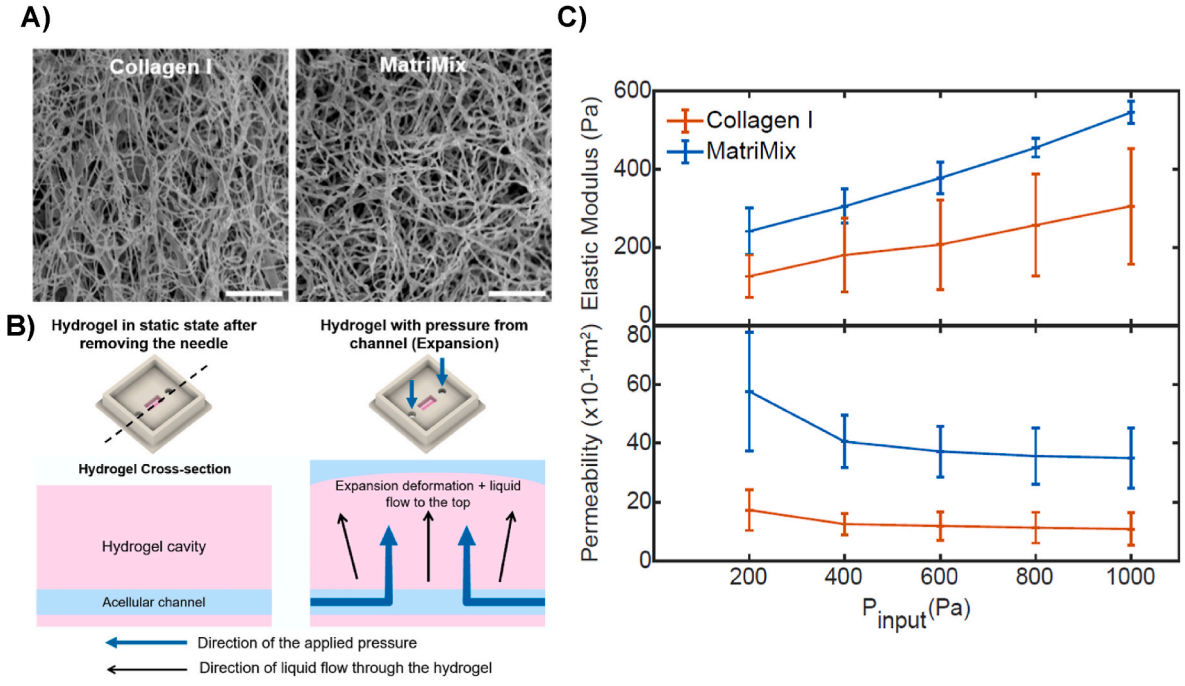

Fig. 2. Physical characterization of Collagen I and MatriMix gels. A) SEM images of Collagen I and MatriMix hydrogels; scale bars: 2 μm. **B)** Basic principle of the pressure measurement performed in the hydrogels. **C)** Hydrogel one-dimensional elastic modulus (top) and permeability (bottom) as function of the input pressure in the channel (n = 3 each).

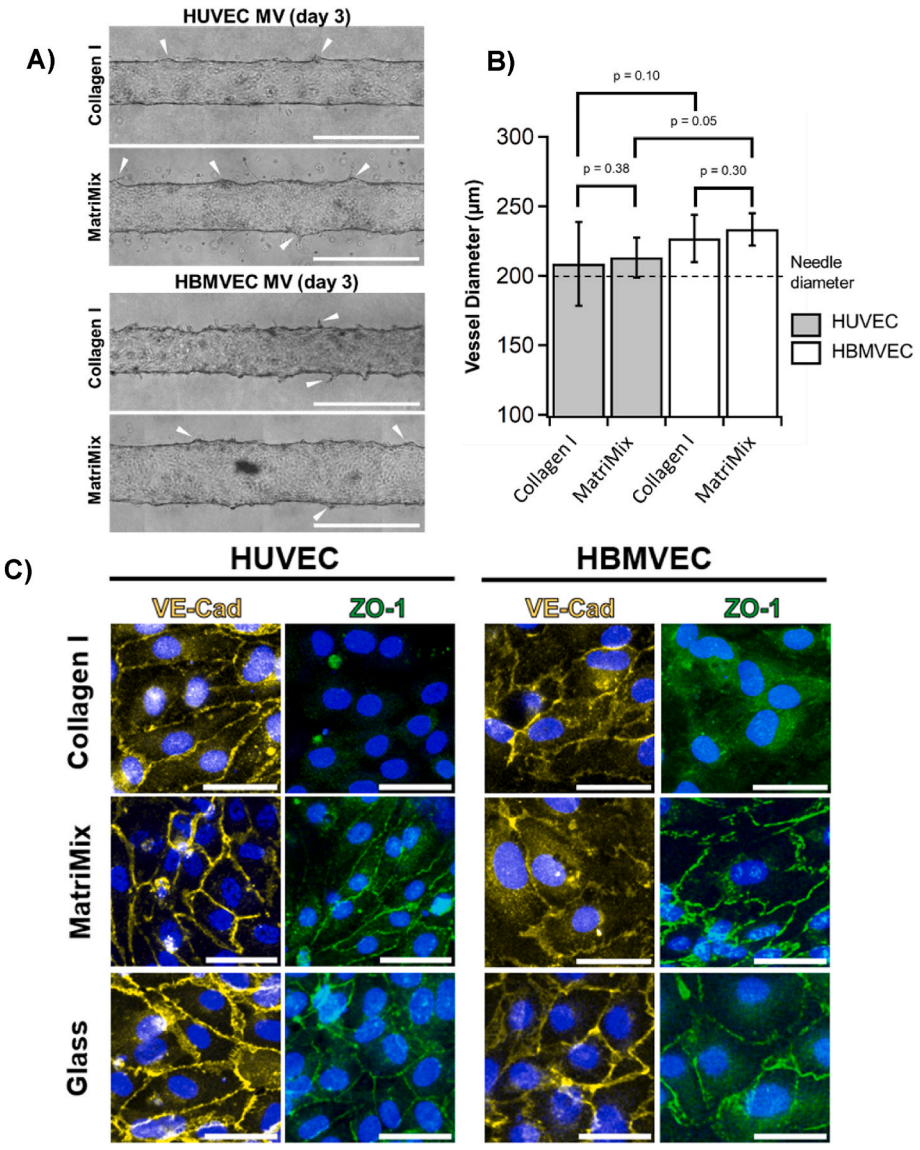

Fig. 3. MV formation and EC-EC junction expression. A) Representative microscopic images of the four EC–hydrogel pairs. Arrowheads point towards possible angiogenesis areas; scale bars: 500 µm. **B)** Average diameter value measured from phase contrast images (n = 5 each). **C)** CLSM images of immunostained VE-Cadherin and ZO-1 immunostaining of each EC–hydrogel combination MV and 2D EC culture on glass substrate. Cell nuclei are stained in blue. Junction colors were modified during image processing; scale bars: 40 µm. See supplementary Data 2 for lower magnified images. (For interpretation of the references to color in this figure legend, the reader is referred to the Web version of this article.)

when relevant for the discussion. $P < 0.05$ was considered statistically significant.

3. Results

3.1. Collagen I and MatriMix have comparable mechanical and diffusion properties

We employed a VoC model to investigate the influence of supporting hydrogels on endothelium barrier function (Fig. 1A and B). The luminal structure of Collagen I or MatriMix, a composite of collagen type I/III with laminin 111 and hyaluronan, components also found in the basement membrane of brain vessels and in the brain ECM [11,18,19], were endothelialized with HUVECs or HBMVECs to form MVs.

SEM observation revealed that the fiber bundles in MatriMix were slightly thicker and their volume fraction lower than those in Collagen I (Fig. 2A). A linear increase of the elastic modulus with the pressure load was observed, characteristic of strain-stiffening collagen hydrogels (Fig. 2B and C). MatriMix was slightly stiffer than Collagen I, although both materials were characterized by a low elastic modulus in the range of 200–600 Pa and 100–500 Pa, respectively. Furthermore, the permeability of both hydrogels remained rather constant for pressures above 400 Pa, with values of 40×10^{-14} m^2 and 16×10^{-14} m^2 for Collagen I and MatriMix, respectively. Both measurements were in excellent agreement with the apparent fiber density and pore size observed in the SEM images.

We measured the diffusion coefficients of two dextran molecules with different molecular weight (4 kDa and 70 kDa) through both hydrogels. We obtained highly similar results at 228 ± 13 and 222 ± 7 µm^2/s for the 4-kDa dextran and 52 ± 7 and 52 ± 3 µm^2/s for the 70-kDa dextran, in Collagen I and MatriMix respectively. These calculations were calibrated by finite element simulations (COMSOL). Fluorescence recovery after photobleaching (FRAP) revealed that the diffusion coefficients of the 4 kDa and 70 kDa probes were 288 ± 13 and 70 ± 7 µm^2/s in buffer solution, respectively (Supplementary Data 1). The diffusive delay induced by the hydrogels was comparable for both

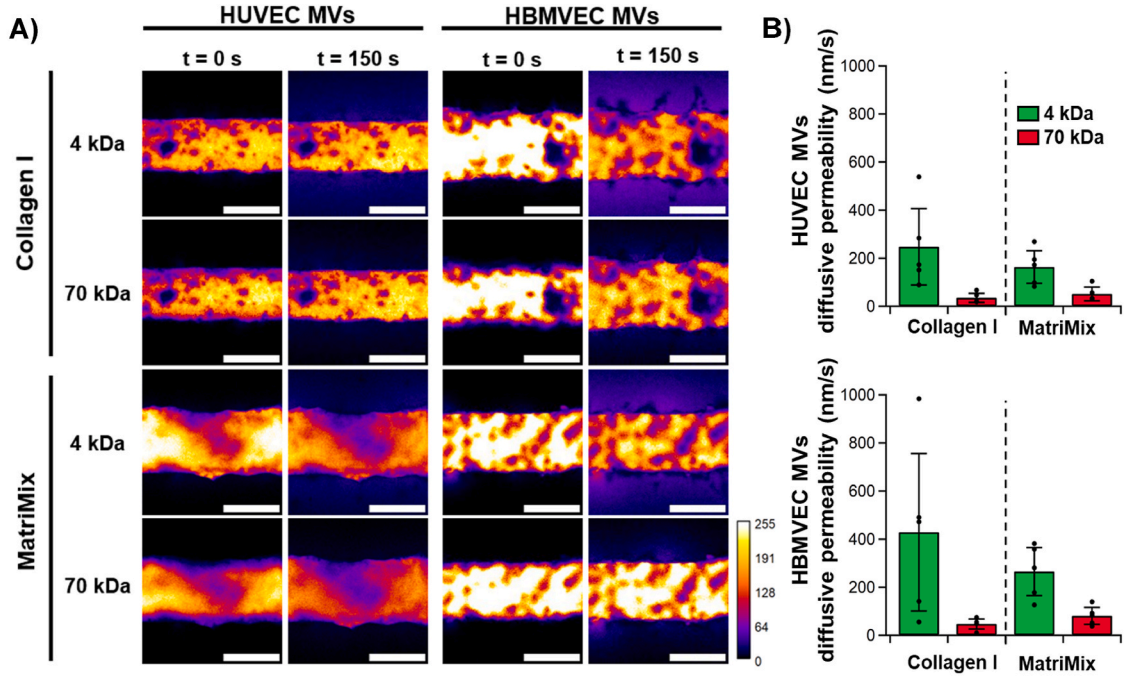

C)

EC type / Hydrogel	P_D (4 kDa) [nm/s]	P_D (70 kDa) [nm/s]	MV selectivity as P_D ratio (4 kDa / 70 kDa)
HUVEC/Collagen I	240 ± 146	35 ± 17	6.9
HUVEC/MatriMix	175 ± 58	58 ± 30	3.7
HBVMEC/Collagen I	429 ± 327	47 ± 21	9.1
HBMVEC/MatriMix	265 ± 100	81 ± 36	3.9

Fig. 4. MV permeability assay A) CLSM images of the diffusion of the two kinds of dextran probes (4 and 70 kDa) immediately after dextran injection (0 s) and 150 s after. Color bar indicates pixel intensity; scale bars: 200 μm. **B)** Calculation of MV P_D for each EC–hydrogel combination (n = 5 each) and expressed as mean ± standard deviation. Individual values are indicated as black markers. **C)** Diffusive permeabilities of each EC–hydrogel combination expressed as mean ± standard deviation. Average MV selectivity, as 4 kDa vs 70 kDa ratio is also indicated. (For interpretation of the references to color in this figure legend, the reader is referred to the Web version of this article.)

hydrogels and was justified by the opposite variations in fiber density and diameter observable in the SEM images. Based on the ratio of diffusion coefficients obtained, the porosity of both hydrogels was approximately 0.77. Altogether, our findings confirm the formation of bundled soft hydrogels for Collagen I and MatriMix with comparable physical properties.

3.2. MatriMix MVs express ZO-1 and tend to have larger diameters

We fabricated MVs containing either HUVECs or HBMVECs to investigate the impact of a change in composition on MV formation and function. After 3 days of culture, MV maturation was sufficient to develop what resembled sprouting angiogenic areas in all EC–hydrogel pairs (Fig. 3A). The ECs also modified the initial diameter during the culture period. MV diameter values varied between 170 and 250 μm on the third day of culture (Fig. 3B), with a tendency toward a larger diameter in HBMVEC MVs than in HUVEC MVs and, within the same EC type, a tendency toward a larger MV diameter with MatriMix.

To visualize how the hydrogel influences the junctions between ECs, MVs were immunostained, targeting either adherent junction VE-cadherin or tight junction-associated protein ZO-1. VE-cadherin junctions were observed in MVs of all EC-hydrogel pairs. On the contrary, ZO-1 tight junction expression was exclusively observed in MVs fabricated in MatriMix for both HUVEC and HBMVEC MVs (Fig. 3C and Supplementary Data 2). These results verify the enhanced biological relevance of the MVs produced using MatriMix compared with those produced from Collagen I alone.

3.3. Collagen I MVs have a higher average permeability than MatriMix MVs

To investigate the barrier function of the MVs, the diffusive permeability (P_D) of the two dextran probes FITC-dextran (4 kDa) and rhodamine-dextran (70 kDa) were simultaneously evaluated via CLSM (Fig. 4A). HBMVEC MVs had a higher average P_D than HUVEC MVs. However, both HBMVEC and HUVEC MVs displayed a wider range of barrier qualities when cultured in Collagen I than in MatriMix (Fig. 4B and C). MV barrier selectivity, defined as the MV permeability to low molecular weight vs. to high molecular weight, is higher in Collagen I MVs as seen by the average ratio between P_D (4 kDa) vs. P_D (75 kDa).

4. Discussion

We investigated the effects of the composition of the supporting hydrogel on the function of 3D HUVEC or HBMVEC MVs *in vitro*. The use of Collagen I was based on its popularity in the field of VoC models, whereas MatriMix presents a better representation of the brain ECM by including laminin and hyaluronan. The physical and structural characterization of both hydrogels revealed their fibrous nature and high deformability, which was associated with a stiffness that typically matched that of the brain ECM of 0.2–1.2 kPa, as inferred from indentation-based techniques [20,21]. Thus, these two materials seemed to mostly differ in composition rather than in physical properties.

MV development after three days was sufficient to show a cohesive layer of human ECs throughout the entire hydrogel channel with some apparent angiogenic areas (Fig. 3A). ZO-1 expression of MV in MatriMix can influence the forces ECs exert on the substrate, which explains the tendency of those MVs to have larger diameter [22] (Fig. 3B and C). On the contrary, VE-cadherin was observed in all EC–hydrogel pairs, consistent with the observation that the matrix composition influences mechano-sensitive pathways in ECs [23,24], as well as junction proteins. This idea is reinforced from our 2D in glass culture images, a standard practice where EC-EC interactions seem to be simplified, where ECs are also capable of producing ZO-1.

We studied the diffusion across the MV barrier of 4 and 70 kDa probes, simulating the behavior of small molecules leaking across the barrier, such as the widely studied beta-amyloid peptides (4.3 kDa) [25], and larger proteins, such as hemoglobin (64.5 kDa) [26]. The diffusive permeability assay indicated enhanced barrier function for both HUVEC and HBMVECs MVs in MatriMix (Fig. 4). Yet, the obtained permeability values for large molecules (70 kDa, approx. 35–80 nm/s) were 23–53 times higher than those of *in vivo* cerebral microvessels (70 kDa, 1.5 nm/s) but comparable with similar VoC models [27,28], suggesting the necessity to combine this approach with co-culture models.

Considering that ZO-1 expression is expected to restrict intercellular junctions [29], our experiments provide insight into whether and how this protein alters endothelial barrier function. ZO-1 induces the reduction of the average P_D and enhances the reproducibility of similar MVs by reducing variability and promoting more stable MV barriers. However, ZO-1 does not appear to influence the selectivity of the MV barrier. MV barrier selectivity decreases between Collagen I MVs (not expressing ZO-1) and MatriMix MVs (expressing ZO-1). We explain this with the hypotheses that Collagen I MVs present small but frequent pores, allowing 4 kDa dextran molecules to diffuse easier than the 70 kDa dextran molecules. Conversely, the tightening of small pores by ZO-1 would increase the contribution of larger holes which reduce the selectivity in MatriMix MVs, while reducing the global P_D value at the same time. Proof of this is that MVs in MatriMix showed higher local variability of 70 kDa P_D, coherent to the existence of less frequent but larger holes than in MVs in Collagen I (Supplementary Data 3).

ECM specifically influences the phenotype of capillary vasculatures [30]. Therefore, the necessity to include or not organ-specific components in the hydrogels is a timely discussion in the VoC field. Indeed, VoCs typically recreate microvasculatures that are in contact with the supporting hydrogel, which plays a crucial role in determining EC phenotype and VoC function [31]. While not achieving BBB-like levels of MV permeability and selectivity, our data support the need to complement hydrogels to emulate organ-specific functions. We suggest that the recent publication of the public Matrisome DataBase [32] may facilitate the design of composite hydrogels for biochemically accurate organ-specific VoC models. We hope for the development of easy-to-handle composite hydrogels, such as MatriMix, for the normalization and characterization of VoCs.

In summary, this study emphasized the relevance of using hydrogels containing ECM components from the target tissue to prepare VoCs with organ-specific traits. Our data demonstrated that only MVs cultured in the hydrogel that contained laminin and hyaluronan, two ECM proteins present in basal membrane and the brain ECM, expressed localized ZO-1, showed reproducible and improved barrier function. However, the endothelial barrier selectivity was not improved in our data, falling short compared to the real BBB. We therefore suggest including this type of hydrogel along with other more commonly-practiced techniques for organ-specific VoC model design, such as shear stress stimuli or coculture with other organ-specific cell types.

CRediT authorship contribution statement

Daniel Alcaide: Writing – review & editing, Writing – original draft, Investigation, Funding acquisition, Formal analysis, Data curation. **Baptiste Alric:** Writing – original draft, Formal analysis, Data curation. **Jean Cacheux:** Writing – review & editing, Software, Methodology. **Shizuka Nakano:** Writing – review & editing, Methodology, Data curation. **Kotaro Doi:** Writing – review & editing, Methodology. **Marie Shinohara:** Writing – review & editing, Methodology. **Makoto Kondo:** Writing – review & editing, Methodology. **Aurelien Bancaud:** Writing – review & editing, Supervision, Methodology. **Yukiko T. Matsunaga:** Writing – review & editing, Supervision, Funding acquisition, Conceptualization.

Declaration of competing interest

The authors declare that they have no known competing financial interests or personal relationships that could have appeared to influence the work reported in this paper.

Acknowledgments

This research was partly supported by WINGS-QSTEP (D.A.), LIMMS, and ARIM of the MEXT, Grant Number: JPMXP1223UT-0331. We also thank Nippi Inc. for providing materials of the culture substrates: collagen, hyaluronan, and laminin-111 E8 in preparation of MatriMix 111.

Appendix A. Supplementary data

Supplementary data to this article can be found online at https://doi.org/10.1016/j.bbrc.2024.150234.

References

[1] J.B. Bassingthwaighte, C.Y. Wang, I.S. Chan, Blood-tissue exchange via transport and transformation by capillary endothelial cells, Circ. Res. (Oct. 1989), https://doi.org/10.1161/01.RES.65.4.997.

[2] I.B. Wilkinson, C.M. McEniery, Arterial stiffness, endothelial function and novel pharmacological approaches, Clin. Exp. Pharmacol. Physiol. 31 (11) (2004) 795–799, https://doi.org/10.1111/j.1440-1681.2004.04074.x.

[3] M. Rothbauer, et al., A decade of organs-on-a-chip emulating human physiology at the microscale: a critical status report on progress in toxicology and pharmacology, Micromachines 12 (5) (May 2021), https://doi.org/10.3390/mi12050470. Art. no. 5.

[4] A.M.A.O. Pollet, J.M.J. den Toonder, Recapitulating the vasculature using organ-on-chip technology, Bioengineering 7 (1) (Mar. 2020), https://doi.org/10.3390/bioengineering7010017. Art. no. 1.

[5] H. Uwamori, Y. Ono, T. Yamashita, K. Arai, R. Sudo, Comparison of organ-specific endothelial cells in terms of microvascular formation and endothelial barrier functions, Microvasc. Res. 122 (Mar. 2019) 60–70, https://doi.org/10.1016/j.mvr.2018.11.007.

[6] S. Maji, H. Lee, Engineering hydrogels for the development of three-dimensional in vitro models, Int. J. Mol. Sci. 23 (5) (Jan. 2022), https://doi.org/10.3390/ijms23052662. Art. no. 5.

[7] L. Santos, et al., Extracellular stiffness modulates the expression of functional proteins and growth factors in endothelial cells, Adv. Healthcare Mater. 4 (14) (2015) 2056–2063, https://doi.org/10.1002/adhm.201500338.

[8] D.A. Chistiakov, A.N. Orekhov, Y.V. Bobryshev, Effects of shear stress on endothelial cells: go with the flow, Acta Physiol. 219 (2) (2017) 382–408, https://doi.org/10.1111/apha.12725.

[9] L.A. Herron, C.S. Hansen, H.E. Abaci, Engineering tissue-specific blood vessels, Bioeng. Transl. Med. 4 (3) (2019) e10139, https://doi.org/10.1002/btm2.10139.

[10] N. Weiss, F. Miller, S. Cazaubon, P.-O. Couraud, The blood-brain barrier in brain homeostasis and neurological diseases, Biochim. Biophys. Acta BBA - Biomembr. 1788 (4) (Apr. 2009) 842–857, https://doi.org/10.1016/j.bbamem.2008.10.022.
[11] N. George, H.M. Geller, Extracellular matrix and traumatic brain injury, J. Neurosci. Res. 96 (4) (2018) 573–588, https://doi.org/10.1002/jnr.24151.
[12] P.A. Soden, A.R. Henderson, E. Lee, A microfluidic model of AQP4 polarization dynamics and fluid transport in the healthy and inflamed human brain: the first step towards glymphatics-on-a-chip, Adv. Biol. 6 (12) (2022) 2200027, https://doi.org/10.1002/adbi.202200027.
[13] J. Pauty, et al., A 3D tissue model-on-a-chip for studying the effects of human senescent fibroblasts on blood vessels, Biomater. Sci. 9 (1) (2021) 199–211, https://doi.org/10.1039/D0BM01297A.
[14] J. Cacheux, et al., Protocol for fabricating and characterizing microvessel-on-a-chip for human umbilical vein endothelial cells, STAR Protoc. 5 (2) (Jun. 2024) 102950, https://doi.org/10.1016/j.xpro.2024.102950.
[15] J. Cacheux, et al., Asymmetry of tensile versus compressive elasticity and permeability contributes to the regulation of exchanges in collagen gels, Sci. Adv. 9 (31) (Aug. 2023) eadf9775, https://doi.org/10.1126/sciadv.adf9775.
[16] K. Takahashi, et al., CD40 is expressed in the subsets of endothelial cells undergoing partial endothelial–mesenchymal transition in tumor microenvironment, Cancer Sci. 115 (2) (2024) 490–506, https://doi.org/10.1111/cas.16045.
[17] J. Cacheux, et al., Endothelial tissue remodeling induced by intraluminal pressure enhances paracellular solute transport, iScience 26 (7) (Jul. 2023) 107141, https://doi.org/10.1016/j.isci.2023.107141.
[18] S.K. Halder, A. Sapkota, R. Milner, The importance of laminin at the blood-brain barrier, Neural Regen. Res. 18 (12) (Dec. 2023) 2557, https://doi.org/10.4103/1673-5374.373677.
[19] R. Rauti, N. Renous, B.M. Maoz, Mimicking the brain extracellular matrix in vitro: a review of current methodologies and challenges, Isr. J. Chem. 60 (12) (2020) 1141–1151, https://doi.org/10.1002/ijch.201900052.
[20] D.C. Stewart, A. Rubiano, K. Dyson, C.S. Simmons, Mechanical characterization of human brain tumors from patients and comparison to potential surgical phantoms, PLoS One 12 (6) (Jun. 2017) e0177561, https://doi.org/10.1371/journal.pone.0177561.
[21] M. Khoonkari, D. Liang, M. Kamperman, F.A.E. Kruyt, P. van Rijn, Physics of brain cancer: multiscale alterations of glioblastoma cells under extracellular matrix stiffening, Pharmaceutics 14 (5) (May 2022), https://doi.org/10.3390/pharmaceutics14051031. Art. no. 5.
[22] A.J. Haas, et al., ZO-1 guides tight junction assembly and epithelial morphogenesis via cytoskeletal tension-dependent and -independent functions, Cells 11 (23) (Jan. 2022), https://doi.org/10.3390/cells11233775. Art. no. 23.
[23] C. Collins, et al., Haemodynamic and extracellular matrix cues regulate the mechanical phenotype and stiffness of aortic endothelial cells, Nat. Commun. 5 (1) (Jun. 2014) 3984, https://doi.org/10.1038/ncomms4984.
[24] J.Y.-J. Shyy, S. Chien, Role of integrins in endothelial mechanosensing of shear stress, Circ. Res. 91 (9) (Nov. 2002) 769–775, https://doi.org/10.1161/01.RES.0000038487.19924.18.
[25] W. Zhang, et al., Blood-brain barrier transport of amyloid beta peptides in efflux pump knock-out animals evaluated by in vivo optical imaging, Fluids Barriers CNS 10 (1) (Feb. 2013) 13, https://doi.org/10.1186/2045-8118-10-13.
[26] H.H. Billett, Hemoglobin and hematocrit, in: H.K. Walker, W.D. Hall, J.W. Hurst (Eds.), Clinical Methods: the History, Physical, and Laboratory Examinations, third ed., Butterworths, Boston, 1990 [Online]. Available: http://www.ncbi.nlm.nih.gov/books/NBK259/. (Accessed 29 April 2024).
[27] W. Yuan, Y. Lv, M. Zeng, B.M. Fu, Non-invasive measurement of solute permeability in cerebral microvessels of the rat, Microvasc. Res. 77 (2) (Mar. 2009) 166–173, https://doi.org/10.1016/j.mvr.2008.08.004.
[28] W.J. Polacheck, M.L. Kutys, J.B. Tefft, C.S. Chen, Microfabricated blood vessels for modeling the vascular transport barrier, Nat. Protoc. 14 (5) (May 2019) 1425–1454, https://doi.org/10.1038/s41596-019-0144-8.
[29] O. Tornavaca, et al., ZO-1 controls endothelial adherens junctions, cell–cell tension, angiogenesis, and barrier formation, J. Cell Biol. 208 (6) (Mar. 2015) 821–838, https://doi.org/10.1083/jcb.201404140.
[30] W.C. Aird, Mechanisms of endothelial cell heterogeneity in health and disease, Circ. Res. 98 (2) (Feb. 2006) 159–162, https://doi.org/10.1161/01.RES.0000204553.32549.a7.
[31] L. Gifre-Renom, M. Daems, A. Luttun, E.A.V. Jones, Organ-specific endothelial cell differentiation and impact of microenvironmental cues on endothelial heterogeneity, Int. J. Mol. Sci. 23 (3) (Jan. 2022), https://doi.org/10.3390/ijms23031477. Art. no. 3.
[32] X. Shao, I.N. Taha, K.R. Clauser, Y. Tom Gao, A. Naba, MatrisomeDB: the ECM-protein knowledge database, Nucleic Acids Res. 48 (D1) (Jan. 2020) D1136–D1144, https://doi.org/10.1093/nar/gkz849.